

Global-QSGD: Practical Floatless Quantization for Distributed Learning with Theoretical Guarantees

Jihao Xin
KAUST*
Saudi Arabia

Marco Canini
KAUST
Saudi Arabia

Peter Richtárik
KAUST
Saudi Arabia

Samuel Horváth
MBZUAI†
United Arab Emirates

Abstract

Efficient distributed training is a principal driver of recent advances in deep learning. However, communication often proves costly and becomes the primary bottleneck in these systems. As a result, there is a demand for the design of efficient communication mechanisms that can empirically boost throughput while providing theoretical guarantees. In this work, we introduce Global-QSGD, a novel family of quantization operators, engineered to accelerate distributed training based on global scaling. We demonstrate that Global-QSGD is the first theoretically rigorous Allreduce-compatible compression mechanism that achieves a provable speed-up by striking a balance between compression error and communication savings. Importantly, Global-QSGD does not rely on costly error feedback due to its inherent unbiasedness and offers up to $\mathcal{O}(\sqrt{n})$ additional compression ratio compared to the popular QSGD quantization (n represents the number of workers). To obtain theoretical guarantees, we generalize the notion of standard unbiased compression operators to incorporate Global-QSGD. We show that this wider class permits standard analysis for unbiased compressors and thus ensures convergence for popular optimization algorithms (e.g., distributed SGD) under typical settings. For the empirical component of our work, we carry out a performance modeling analysis to determine if Global-QSGD can enhance training throughput under specific hardware configurations. We also conduct extensive empirical evaluations on various tasks, testing our theory on both NVLink and PCIe connections as well as a large-scale cloud system.

1 Introduction

Recent progress in deep learning has been driven by building large, sophisticated models on ever-increasing data sets. However, this comes with the cost of longer training times, which can take days or even weeks [1–4]. A common way to reduce training time is to employ distributed training [5, 6], where data is distributed among large-scale clusters with numerous nodes. Then, we can formulate the learning objective as the minimization problem over the average of n functions:

$$\min_{x \in \mathbb{R}^d} \left[f(x) \stackrel{\text{def}}{=} \frac{1}{n} \sum_{i=1}^n f_i(x) \right] \quad \text{where} \quad f_i(x) \stackrel{\text{def}}{=} \mathbf{E}_{\xi_i \sim \mathcal{D}_i} [f_i(x, \xi_i)], \quad (1)$$

where f_i corresponds to the local loss on node $i \in \{1, 2, \dots, n\}$ and d is the dimensionality of the model. Each node has access to a partition of the training dataset, indicated by \mathcal{D}_i . This approach is known as *data-parallelism*. The most popular technique to solve this objective is the parallel distributed SGD algorithm that updates the current estimate of the solution using gradient information. Formally, we write $x^{k+1} = x^k - \eta^k \frac{1}{n} \sum_{i=1}^n \nabla f_i(x, \xi_i)$.

*King Abdullah University of Science and Technology

†Mohamed bin Zayed University of Artificial Intelligence

Table 1: Conceptual comparison of our methods to the relevant literature.

Algorithm	Supports Allreduce	Provably works	Works w/o EF	Large Comp. Ratio	Tunable Compression	Reference
Global-QSGD	✓ ⁽¹⁾	✓	✓	✓/✗ ⁽³⁾	✓	Ours
INTSGD (theor.)	✓	✓	✓	✗	✗	[28]
INTSGD (pract.)	✓	✗	✓	✗	✗	[28]
POWERSGD (theor.)	✓	✓	✗	✓	✓	[9]
POWERSGD (pract.)	✓	✗	✗	✓	✓	[9]
NATSGD	✗	✓	✓	✗	✗	[19]
QSGD	✗	✓	✓	✓	✓	[14] ⁽²⁾
SIGNSGD	✗	✓	✗	✗	✗	[29]

(1) Except in the case that the vector is in a sparse representation.

(2) Originally proposed by Alistarh et al. [14], but we consider more general version that allows arbitrary quantization levels analyzed by Horváth et al. [19].

(3) Large comp. ratio is only possible for Allgather since for Allreduce, we communicate dense vectors.

Communication bottleneck in ML training. Increasing model and data set sizes make training extensively computationally demanding. Thankfully, there has been steady progress in improving computation performance over the last decade, mainly due to accelerators like GPUs or TPUs [7]. On the other hand, network advances lack behind, making the communication-intensive model update, i.e., the synchronization step, a key performance bottleneck. For instance, Sapio et al. [8] shows that for popular deep neural network benchmarks and deployments, communication can take more than 90% of the total training time without much possibility to overlap computation and communication, which significantly limits the benefits of extra compute capabilities due to distributed training.

Gradient synchronization protocols. The two standard protocols for gradient synchronization are Allreduce and Allgather aggregation, which may use either Parameter Server or peer-to-peer communication under the hood. The main distinction between them is that Allgather communicates all vectors, while Allreduce exploits associativity of addition to rewrite the computation of sum as $(g_1 + g_2) + (g_3 + g_4)$, which enables to apply a divide-and-conquer approach and allows the summation operation to be split across multiple nodes; see Appendix C for a visualization. This allows for better scalability in terms of cluster workers, since both the computation and the communication scale as $\tilde{O}(n)$ for Allreduce, compared to $O(n^2)$ for Allgather. For this reason, current distributed deep learning algorithms predominantly use Allreduce as the default communication primitive [9, 10]. Allgather is widely used in scenarios where both g_1 and g_2 are cheap to communicate, but their sum is not, e.g., sum of two sparse vectors with non-overlapping non-zero coordinates [11].

1.1 Related Work

Table 1 lists a comprehensive comparison of the related methods.

Communication compression. A popular approach to remedy the previously discussed network bottleneck is to reduce the size of messages (typically gradient vectors; see (1)) transmitted between the nodes [12–15]. These techniques rely on lossy compression of the messages. In the most basic form, these schemes decrease the number of bits to represent floating point numbers [16, 17], reducing the size of a d -dimensional (gradient) vector by a constant factor. Quantization approaches attain up to $O(\sqrt{d})$ compression [12, 14, 15, 18, 19]. The most aggressive sparsification schemes reach $O(d)$ compression by only sending a constant number of bits per iteration [20–24]. An alternative approach is to not compute the gradient at first and subsequently compress it, but to update only a subset of elements of the iterate x using coordinate descent type updates [25–27].

In general, there are two classes of compressor operators commonly considered in literature—unbiased and biased compressors. Unbiased compressors with relatively bounded variance (i.e., Definition 2.1) are usually easy to analyze as unbiased compression can be seen as an extra variance to the update during the aggregation; see [30] for details. For biased compressors (e.g., Top- k [22], SIGNSGD [31], POWERSGD [9]), one needs to employ some correction mechanism to ensure the convergence [32]. For instance, the error-feedback (EF) mechanism [23, 29, 33] and the induced compressor (IC) [34] fix the convergence. This comes with the price as EF requires extra memory and does not work with non-smooth functions and IC relies on the second compressor that is unbiased.

Finally, as already discussed, Allreduce is usually the communication backbone of distributed training. Unfortunately, most of the previously mentioned compressors are not naively compatible with this

communication primitive since the sum of two compressed vectors is not an inexpensive operation (i.e., it requires custom format conversions and/or aggregation logic). This includes greedy and random sparsifiers,³ quantization, and sign-based methods. To the best of our knowledge, the only compressors compatible with Allreduce are POWERSGD [9] and INTSGD [8, 28]. However, practical implementations for these methods are only heuristics, i.e., they do not come with rigorous theoretical guarantees.

Increasing the computation to communication ratio. The orthogonal approach is to reduce communication frequency by giving more work to local workers before the update is communicated. This includes increasing mini-batch size [36], defining local problems for each worker [37, 38] or reducing the communication frequency [39–43]. In this work, we focus on communication compression.

1.2 Contributions

- We introduce Global-QSGD, a novel family of quantization methods based on global information with features:
 - **Allreduce Compatible.** Compressed vectors can be aggregated directly by Allreduce.
 - **Unbiased.** Global-QSGD does not require expensive error correction mechanisms.
 - **Higher Compression Ratio** Global-QSGD leads to a compression ratio proportional up to $\mathcal{O}(\sqrt{nd})$, while the previous quantization can only reach $\mathcal{O}(\sqrt{d})$.
 - **Reduced Memory Consumption.** Global-QSGD improves the scaling of the required memory for aggregation from $\mathcal{O}(\log(n))$ to $\mathcal{O}(\log \log(n))$, where n is the number of computing nodes.
 - **Flexible Precision.** Unlike INTSGD, users can choose Global-QSGD’s precision.
- We provide theoretical analysis to establish:
 - **Real Convergence Guarantees.** Global-QSGD is the first Allreduce-compatible compressor that does not require any heuristics [9, 28] in convergence analysis, thus its implementation follows the theoretical guarantees.
 - **Bounded Variance.** Methods that work with an unbiased compressor with bounded variance can seamlessly extend to Global-QSGD with the same rate of convergence. We achieve this by introducing a more general notion of an unbiased distributed mean compression operator with bounded variance.
 - **Performance Modeling.** We analyze what factors influence training throughput and when Global-QSGD is beneficial.
- We conduct extensive empirical validations for real-world tasks on different network fabrics, which achieves $1.38\text{--}3.51\times$ speedups with compression ratio $= \frac{1}{4}$. We also evaluate our methods in a large-scale system (up to 64 GPUs).

2 Unbiased Distributed Mean Compression Operator

We start by introducing used notation. We denote ℓ_p -norms for $y \in \mathbb{R}^d$ as $\|y\|_p \stackrel{\text{def}}{=} (\sum_{i=1}^n |y_i|^p)^{1/p}$ for $p \in (1, \infty)$. For $p = \infty$, $\|y\|_p$ denotes the maximum element of y in terms of magnitude. Let $\mathbf{x} = [x_1, x_2, \dots, x_n] \in \mathbb{R}^{nd}$, where $x_1, x_2, \dots, x_n \in \mathbb{R}^d$. We denote $\|\mathbf{x}\|_{q,p}$ to be a norm on \mathbb{R}^{nd} defined as $\|\mathbf{x}\|_{q,p} \stackrel{\text{def}}{=} (\sum_{i=1}^d \|x_i\|_q^p)^{1/p}$. For any vectors x, y , $x \circ y$ represents their element-wise multiplication, and, for any vector x , $|x|$, $\text{sign } x$ stand for element-wise absolute value and signum operations, respectively. We denote $[n] \stackrel{\text{def}}{=} \{1, 2, \dots, n\}$ for any $n \in \mathbb{N}$. All the missing proofs are provided in Appendix A.

When one analyzes the performance of unbiased compression operators, it is common to consider the following class of unbiased compressor operators [44, 45, 23, 46].

Definition 2.1 (Unbiased Compression Operator). A randomized mapping $\mathcal{C}: \mathbb{R}^d \rightarrow \mathbb{R}^d$ is an *unbiased compression operator (unbiased compressor)* if there exists $\omega \geq 0$ such that $\forall x \in \mathbb{R}^d$:

$$\mathbf{E}[\mathcal{C}(x)] = x, \quad \mathbf{E}[\|\mathcal{C}(x) - x\|_2^2] \leq \omega \|x\|_2^2. \quad (2)$$

³For random sparsifiers, one can share random seeds across workers to make it Allreduce compatible, e.g., see synchronized random seed [35].

If this holds, we will for simplicity write $\mathcal{C} \in \mathbb{U}^n(\omega)$.

In our work, we generalize the above definition to what we refer to as *an unbiased distributed mean compression operator*.

Definition 2.2 (Unbiased Distributed Mean Compression Operator). For any $x_1, x_2, \dots, x_n \in \mathbb{R}^d$, let

$$\mathbf{x} \stackrel{\text{def}}{=} [x_1, x_2, \dots, x_n] \in \mathbb{R}^{nd}, \quad \bar{\mathbf{x}} \stackrel{\text{def}}{=} \frac{1}{n} \sum_{i=1}^n x_i. \quad (3)$$

A randomized mapping $\mathcal{G}: \mathbb{R}^{nd} \rightarrow \mathbb{R}^d$ is an *unbiased distributed mean compression operator* (unbiased distributed mean compressor) if there exists $\theta \geq 0$ such that $\forall \mathbf{x} \in \mathbb{R}^{nd}$:

$$\mathbb{E}[\mathcal{G}(\mathbf{x})] = \bar{\mathbf{x}}, \quad \mathbb{E}[\|\mathcal{G}(\mathbf{x}) - \bar{\mathbf{x}}\|_2^2] \leq \frac{\theta}{n} \|\mathbf{x}\|_{2,2}^2. \quad (4)$$

If this holds, we will for simplicity write $\mathcal{G} \in \mathbb{U}^{n,d}(\theta)$.

To show that Definition 2.2 is more general than Definition 2.1, we provide the following lemma that formalizes this claim.

Lemma 2.3 ($\mathbb{C} \subset \mathbb{U}^{n,d}$). If $\mathcal{C}_1, \mathcal{C}_2, \dots, \mathcal{C}_n \in \mathbb{U}^n(\omega)$ and they are independent, then $\mathcal{G}: \mathbb{R}^{nd} \rightarrow \mathbb{R}^d$ defined as

$$\mathcal{G}(\mathbf{x}) \stackrel{\text{def}}{=} \frac{1}{n} \sum_{i=1}^n \mathcal{C}_i(x_i)$$

belongs to $\mathbb{U}^{n,d}(\omega/n)$.

Equipped with these definitions, we are ready to proceed with the main results.

3 Global-QSGD

One of our main contributions is a proposal of new compression operators that is based on quantization operators [14, 19, 47], where the main difference is that we propose to normalize by a norm of the global vector $\|\mathbf{x}\|_{q,p}$ instead of each client using its local norm $\|x_i\|_p$. The formal definition follows.

Definition 3.1 (Global-QSGD (Global-Q)). The Global-QSGD operator with respect to the p norm and with s levels

$$0 = l_s < l_{s-1} < l_{s-2} < \dots < l_1 < l_0 = 1,$$

denoted $\text{Global-Q}_l^{q,p}$, is defined as follows. Let $\mathbf{x} = [x_1, x_2, \dots, x_n] \in \mathbb{R}^{nd}$. Let $y_i \stackrel{\text{def}}{=} |x_i| / \|\mathbf{x}\|_{q,p} \in \mathbb{R}^d$ for all $i \in [n]$. Then

$$\text{Global-Q}_l^{q,p}(\mathbf{x}) \stackrel{\text{def}}{=} \|\mathbf{x}\|_{q,p} \frac{1}{n} \sum_{i=1}^n \text{sign}(x_i) \circ \xi_i(y_i), \quad (5)$$

where $\xi_i(y_i)$ is an independent element-wise random rounding operator such that

$$(\xi_i(y_i))_j \stackrel{\text{def}}{=} \begin{cases} l_{u_i^j} & \text{with probability } \frac{(y_i)_j - l_{u_i^j+1}}{l_{u_i^j} - l_{u_i^j+1}}, \\ l_{u_i^j+1} & \text{otherwise} \end{cases}, \quad (6)$$

for $j \in [d]$, where $u_i^j \in \{0, 1, 2, \dots, s\}$ is such that $l_{u_i^j} \leq (y_i)_j \leq l_{u_i^j+1}$.

In the next lemma, we show that $\text{Global-Q}_l^{q,p} \in \mathbb{U}^{n,d}(\theta)$ and an interesting reduction property of the $\text{Global-Q}_l^{q,p}$ compression operator that helps us to analyze its theoretical properties using known results for the case $n = 1$ [14, 19].

Lemma 3.2. Let $\mathcal{Q}_l^{q,p}(\mathbf{x}) \stackrel{\text{def}}{=} \|\mathbf{x}\|_{q,p} \text{sign}(\mathbf{x}) \circ \xi(\mathbf{y})$, where $\xi(\mathbf{y}) = [\xi_1(y_1), \xi_2(y_2), \dots, \xi_n(y_n)]$ and $\xi_i(y_i)$ is defined in (6). Then,

$$\text{Global-Q}_l^{q,p}(\mathbf{x}) = \frac{1}{n} \sum_{i=1}^n (\mathcal{Q}_l^{q,p}(\mathbf{x}))_i, \quad (7)$$

where $(\mathcal{Q}_l^{q,p}(\mathbf{x}))_i$ refers to coordinates $[(i-1)d+1, \dots, id]$. Moreover, if $\mathcal{Q}_l^{q,p} \in \mathbb{C}(\omega)$ then $\text{Global-Q}_l^{q,p} \in \mathbb{U}^{n,d}(\theta)$ with $\theta = \omega/n$.

Note that there is a difference in the dependence on the dimension, i.e., $d \rightarrow nd$, since we work with the concatenated vector \mathbf{x} .

We consider two forms of Global- $\mathcal{Q}_l^{q,p}$ with different partitions of $[0, 1]$ interval. Firstly, **standard dithering** with uniform quantization levels, i.e., $l_i = s^{-i}/s$ for $i \in \{0, 1, \dots, s\}$, denoted by Global- $\mathcal{L}_s^{q,p}$, and, secondly, **exponential dithering** with exponentially spaced levels, i.e., $l_s = 0$ and $l_i = 1/2^{s-i}$ for $i \in \{1, \dots, s\}$, denoted by Global- $\mathcal{E}_s^{q,p}$ ⁴

Next, we derive the exact bound on the variance of both Global- $\mathcal{L}_s^{q,p}$ and Global- $\mathcal{E}_s^{q,p}$. In addition, for the special case of $p = q = 2$, we can bound sparsity, i.e., the sum of zero norms of the communicated vectors ($\|y\|_0$ denotes the number of non-zero elements of y).

Theorem 3.3. *If $p, q \geq 2$ then Global- $\mathcal{L}_s^{q,p} \in \mathbb{U}^{n,d}(\frac{\sqrt{d}}{\sqrt{ns}})$ for $s \leq \sqrt{nd}$, and Global- $\mathcal{L}_s^{q,p} \in \mathbb{U}^{n,d}(\frac{1}{8n} + \frac{\sqrt{d}}{\sqrt{n2^{s-1}}})$ for $s \leq 1 + \log(\sqrt{nd})$. Moreover, if $p = q = 2$ then for any $\mathbf{x} \in \mathbb{R}^{nd}$*

$$\sum_{i=1}^n \|(\mathcal{L}_s^{2,2}(\mathbf{x}))_i\|_0 \leq s^2 + \sqrt{nd} \quad \text{and} \quad \sum_{i=1}^n \|(\mathcal{E}_s^{2,2}(\mathbf{x}))_i\|_0 \leq 2^{2s-2} + \sqrt{nd}.$$

The above theorem guarantees that we can achieve $\mathcal{O}(\sqrt{nd})$ compression ratio for $s = \mathcal{O}(1)$. Furthermore, we note that the variance bound scales better for the exponential dithering with the number of levels s , which means that the exponential dithering exhibits a smaller relative compression error for larger s .

3.1 Communication Protocol

Algorithm 1 gives the pseudo-code of Global-QSGD.

The first step of our quantization procedure is the normalization by the global norm $\|\mathbf{x}\|_{q,p}$. This could be efficiently communicated using $\|\mathbf{x}\|_{q,p} = (\sum_{i=1}^n \|x_i\|_p^q)^{1/p}$, which is compatible with Allreduce of $\{\|x_i\|_p^q\}$. Note that for the case $p = \infty$, we simply apply Allreduce with the maximum operator of $\{\|x_i\|_q\}$ and obtain the desired result. The next step is to communicate $\{\text{sign}(x_i), \xi_i(y_i)\}$. We consider two options here.

Firstly, if we expect $\{\xi_i(y_i)\}$ to be sparse, e.g., $p = q = 2$ and $s = \mathcal{O}(1)$, then we communicate only non-zero coefficients, signs $\{\text{sign}(x_i)\}$ and the quantized normalized values $\{\xi_i(y_i)\}$ of the non-zero elements denoted by nnz_i , $\{\text{sign}(x_i)[nnz_i]\}$ and $\{\text{Encode}(\xi_i(y_i)[nnz_i])\}$, respectively. In this case, we use Allgather as the communication protocol since we communicate sparse vectors, and the sparsity pattern might be different across nodes. For example, if $p = q = 2$ and $s = \mathcal{O}(1)$, the gather call communication complexity is only $\mathcal{O}(n\sqrt{nd})$ since there is in expectation at most $\mathcal{O}(\sqrt{nd})$ non-zero coordinates globally compared to $\mathcal{O}(n^2\sqrt{d})$ for QSGD. Furthermore, if we select $r = \mathcal{O}(\sqrt{n})$, where r is the rank parameter for POWERSGD, the overall communication cost of our method with Allgather is equivalent to POWERSGD with Allreduce. In the dense regime, we do not communicate positions of non-zero elements and communicate full vectors, i.e., $\{\text{sign}(x_i), \xi_i(y_i)\}$. In this case, our floatless compressors can benefit from Allreduce, as we show next. For Global- $\mathcal{L}_s^{q,p}$, we only sum integers, so the output is also an integer. For Global- $\mathcal{E}_s^{q,p}$, Allreduce becomes more complicated as we sum the numbers of the type 2^k , and the sum has to be of the same type in order to apply Allreduce. Therefore, we design stochastic unbiased exponential rounding denoted by \mathcal{C}_{nat} following the notation introduced in [19, Definition 1]. \mathcal{C}_{nat} operation brings an extra small $9/8$ factor of variance in each step. In total, this accounts for $(9/8)^{\#\text{aggregation steps}}$, i.e., $(9/8)^{\log(n)} \leq n^{0.17}$ for Tree-Allreduce. For $n = 16$ or $n = 1024$, this brings a tiny factor of 1.6 and 3.25 of extra variance, respectively. As we show in Appendix B and Algorithm 2, this *reduce* function can be efficiently implemented using simple integer inequalities, additions, and subtractions. Finally, we discuss a strong advantage of the exponential structure of the levels, which is its scaling with respect to the number of nodes n . Let us look at the following example, where we use $\text{int}A$ ($A \in \mathbb{N}$) to represent integers. For INTSGD, we would need to clip all the integers into the $[-2^{A-1}/n, 2^{A-1}-1/n]$ interval

⁴We can work with any basis. We use base 2 for simplicity and the fact that this is naturally compatible with the binary representation of floats.

Algorithm 1 Global-QSGD

```
1: Input: Update  $\mathbf{x} = [x_1, x_2, \dots, x_n]$  distributed among  $n$  machines,  $\text{sparse} \in \{\text{True}, \text{False}\}$ ,  
   Quantization Global- $\mathcal{Q}_l^{q,p}$   
2:  $\|\mathbf{x}\|_p = (\text{Allreduce}(\text{SUM}\{\|x_i\|_p^p\}))^{1/p}$   
3: for  $i \in \{1, 2, \dots, n\}$  do // In parallel  
4:   Compute  $\text{sign}(x_i), \xi_i(y_i)$   
5: end for  
6: if  $\text{sparse}$  then  
7:   Return:  $\frac{1}{n}$  Allgather(  
8:      $\text{SUM}\{\text{nnz}_i, \text{sign}(x_i)[\text{nnz}_i], \xi_i(y_i)[\text{nnz}_i]\}$ )  
9: else  
10:  Return:  $\frac{1}{n}$  Allreduce(  
11:     $\text{SUM}\{\text{sign}(x_i), \xi_i(y_i)\}$ )  
12: end if
```

to avoid possible overflow⁵. Therefore, $1 + \log(n) \leq A$; otherwise, the interval would be empty. This means that for $n \geq 16$, INTSGD can't operate with int4 without possible overflows. In the case of linear quantization levels Global- \mathcal{L}_s^p , the maximum number that we might encounter is ns (if we sum the largest level n times), plus we need to hold one bit for the sign. Therefore, we require $1 + \log(s + 1) + \log(n) \leq A$, which can't be satisfied for any s in the case $n = 16$ and $A = 4$. On the other hand, the maximum number we can encounter with Global- \mathcal{E}_s^p is $n2^s$, but since we only communicate exponent, we obtain improved scaling as the maximum communicated integer is $s + \log(n)$. Therefore, we only require that $1 + \log(s + 1 + \log(n)) \leq A$, which is satisfied for $s \leq 3$. This is because GE_s^p scales as $\log(\log(n))$ with n instead of just $\log(n)$.

3.2 Comparison with INTSGD

The most similar method to our proposed quantization is INTSGD, which also normalizes communicated messages with a global constant, where the main difference is that the normalization factor is computed recursively, while for our methods, the normalization only depends on the current communicated message. Another critical distinction/contribution is that, unlike other methods, our Global-QSGD offers provable convergence guarantees and is *the first method* that can be run as analyzed, i.e., it does not rely on any heuristics that make it practical. For instance, INTSGD requires clipping of communicated integers, and POWERSGD approximates low-rank decomposition with power iteration, plus it relies on memory-expensive error feedback. Finally, we have the freedom to choose levels and precision based on the application.

4 Convergence Guarantees: Variance Decomposition

In this section, we showcase how the standard analysis for unbiased compressors (Definition 2.1) can be generalized to the proposed unbiased distributed mean compression operator (Definition 2.2). Since we assume compressors to be unbiased, the only challenge of the analysis is to bound the variance of the gradient estimator⁶. The proof details are in A.5 We show that, applying the unbiased distributed mean compression operator $\mathcal{Q} \in \mathbb{U}^{n,d}(\theta)$ leads to the same rate as applying unbiased compression operators locally, where ω/n is replaced with θ in the final convergence rate. For the exact convergence rates, we refer the reader to the general analysis of Gorbunov et al. [30]. Using these results, Gorbunov et al. [30] has shown that the worst-case increase in the number of iterations to achieve the same precision as the algorithm without compression is by the factor $1 + \omega$ ([30, Theorem 4.1 for Alg. 1: SGD and Alg. 13: Quantized-SGD] that translates to $1 + \theta n$ for the unbiased distributed mean compression operators. For our exponential dithering, this would be a factor of $1 + n^{1.17} \left(\frac{1}{8n} + \sqrt{d}/\sqrt{n}2^{s-1} \right)$. In this estimate, we consider all the sources of variance for AllReduce, i.e., variance due to initial quantization and extra variance due to stochastic rounding during AllReduce. For example, we consider setup, where we use our exponential dithering to decrease communication precision to 8 from 32 bits and if the dimensionality of the model is

⁵Note that the necessity of clipping makes INTSGD algorithm heuristic with no theoretical guarantees, while as we show next, one can directly control the number of levels s for our methods with no violation of theoretical results.

⁶The same applies to the analysis of non-smooth functions, where gradients are replaced with subgradients.

$n = 10^6$, and the number of machines $n = 16$. We reserve 1 bit to the sign and the other 7 bits to levels. Plugging this into our formula, we obtain that the worst-case increase in the expected number of iterations is 20%, while we save 75% of communication. Therefore, if communication is a significant bottleneck, our quantization leads to provable speed up. In addition, note that this is only the worst-case scenario, and in real-world scenarios, this can be much less, e.g., the empirical compression error in our experiments is below 0.5% for exponential dithering.

5 Performance Model

In general, gradient compression methods can only be beneficial if the introduced computation overhead can be compensated by communication gains. Thus, we propose a performance model to analyze when Global-QSGD can speed up the training. As discussed in Section 1, we use Allreduce for gradient communication. There are two popular Allreduce algorithms: Ring-based and Tree-based Allreduce. We adopt a Tree-based Allreduce, as it has fewer reduction steps, where each quantized reduction introduces computation overhead and accuracy loss due to random rounding.

The tree Allreduce algorithm first recursively aggregates the gradients, then does a recursive-doubling Allgather. The depth of the tree is $2\log(N)$ where N is the size of workers. The performance of Allreduce is well studied [48] and it is commonly modeled as: $2\log(N)\alpha + 2\frac{\log(N)S}{\beta} + \frac{\log(N)S}{\gamma}$, where α is the propagation delay in seconds, S is the size of gradients in bytes, β is the bandwidth (byte/s), and γ is the computation speed (byte/s). The first term represents the propagation delay, the second term is the bidirectional transmission delay, and the last term is the computation cost.

We denote the quantized gradient size as \hat{S} , and the computation cost with custom reduction as $\hat{\gamma}$. The bandwidth and propagation delay remains the same. Denote the quantization & dequantization time is δ factor the gradient size. Then the Allreduce performance after applying Global-QSGD is: $2\log(N)\alpha + 2\frac{\log(N)\hat{S}}{\beta} + \frac{\log(N)\hat{S}}{\hat{\gamma}} + \delta S$.

We denote the quantization ratio $\rho = \frac{S}{\hat{S}} (= 4)$ ⁷. For the computation cost, we observe that the quantization and dequantization operations are executed only once per Allreduce invocation, and so we consider it negligible ($\delta = 0$). Thus, the cost of the reduction operation will dominate the performance as the number of workers increases. We denote the computation overhead as $\omega = \frac{\gamma}{\hat{\gamma}}$. We empirically measure⁸ this overhead to be $\omega_S = 1$ and $\omega_E = \frac{1}{79}$, for standard and exponential dithering, respectively. The reduction operation of standard dithering is the native arithmetic summation, which has a similar time for uint8 and float32 data types in our experiments. Instead, the custom reduction used for exponential dithering involves more arithmetic operations, which yield a higher computation overhead.

$$\beta < \frac{6\omega}{1 - 4\omega}\gamma \quad (8)$$

Our algorithm can speed up training throughput if Equation (8) holds (Proof at A.4).

With $\omega_S = 1$, theoretically, standard dithering is guaranteed to speed up training (since $\beta > 0$). In the case of exponential dithering ($\omega_E = \frac{1}{79}$), there is a training speed up if the relation $\beta < 0.08\gamma$ holds. In Section 7, our evaluation is done using A100 GPU ($\gamma = 2$ TB/s) with NVLink ($\beta = 53.9$ GB/s) or PCIe ($\beta = 5.4$ GB/s), where under both network fabrics the inequality holds.

6 Implementation

For ease of use, we implement Global-QSGD with support for both standard dithering Global- $\mathcal{L}_s^{q,p}$ and exponential dithering Global- $\mathcal{E}_s^{q,p}$, which by default uses the L-infinity norm ($p = q = \infty$), and the gradients are quantized to 8 bits ($s = 255$). The algorithm is wrapped into a custom Allreduce module integrated with the standard PyTorch DDP module as a hook.

Our hook procedure is invoked by PyTorch DDP at the granularity of a gradient bucket, which by default has a size of at least 25 MB. The procedure consists of three steps: Quantization, Allreduce, and Dequantization. In the case of exponential dithering, the Allreduce step uses a custom reduction

⁷Our evaluation by default quantizes from Float32 to 8bits . Global-QSGD also works with other bits.

⁸Measured with 25 MB (PyTorch default communication size) data in one A100 GPU.

function. To create a custom reduction function, we implement a custom Allreduce algorithm using NCCL’s point-to-point asynchronous communication API. We support both ring and tree Allreduce. Quantization, dequantization, and custom reduction are mostly written as optimized CUDA kernel functions and run on the GPU.

We plan to release our code as open source. To use our approach, the user simply needs to load a Python module and register our algorithm by invoking the DDP hook API, like: `model.register_comm_hook(None, exponential_dithering_hook)`.

7 Evaluation

The aim of our evaluation is to illustrate that our proposal is practical and beneficial in a range of scenarios, including with different bandwidths among GPUs. We focus on measuring the run time as well as the speedup in training throughput (samples/s) for benchmarks in three distinct application domains of DL. Through task-specific metrics on the test set, we show that Global-QSGD does not impair the model’s generalization ability. We compare Global-QSGD against the no quantization baseline and with QSGD, PowerSGD and L-Greco⁹ [49]. We further illustrate that, compared to standard dithering, exponential dithering achieves better overall performance thanks to its higher precision and despite its additional overhead due to the custom reduction operation.

Setup. For small-scale experiments, we use one ASUS ESC N4A-E11 server equipped with 4 NVIDIA A100 GPUs, each with 40 GB of RAM. The server runs Ubuntu 22.04 with CUDA 11.6, and we use PyTorch 1.13.0. To tease out the effects of bandwidth on training speed (analyzed in Section 5), we run experiments with two interconnects: NVLink (fast) and PCI-e bus (slow). The GPU to GPU bandwidth¹⁰ is 53.9 GB/s and 5.4 GB/s, respectively. We also run an additional large-scale experiment with 64 servers each having 1 A100 GPU on Google Cloud Platform (Cloud). The servers are connected by a dynamic network with bandwidth varying from 200 Mbps to 1.5 Gbps. For fairness, we substitute NCCL’s Allreduce to our own Allreduce implementation for all evaluations.

Benchmarks. Table 2 lists the three DNN models we use for evaluation.

Task	Model	Dataset	Parameter Size	Training Epochs
Recommendation Model	DeepLight	Tiny Criteo’s Click Prediction	607,959,381	10
Image Classification	ResNet101	MinImageNet	126,886,696	90
Language Model	TransformerXL - 16 layers	WikiText-103	191,950,298	20

Table 2: Summary of the benchmarks used in this work.

Speedup. Figure 1 shows the speedup obtained by Global-QSGD compared to no quantization as the baseline while training different benchmarks on a constant number of epochs. Global-QSGD can achieve up to $3.17\times$ speedup in Cloud, $3.51\times$ with PCIe. Global-QSGD can still achieve $1.38\times$ speedup on NVLink, which has the highest GPU bandwidth.

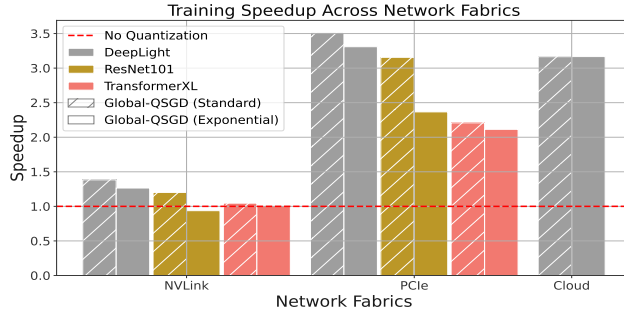


Figure 1: Training throughput speedup normalized to no quantization baseline.

Convergence. Figure 2 shows that Global-QSGD, especially with exponential dithering can preserve convergence. Global-QSGD always achieves the fastest run time, and both exponential dithering and

⁹Based on PowerSGD. Using default hyperparameters: `warmup_steps = 1000`; `adjust_frequency = 1000`; `adjust_beta=4`; `adjust_gamma=0.25`;

¹⁰This is measured for a directed transfer of 25 MB data using the NCCL tests suite.

standard dithering achieve good convergence while striking a different trade-off between run time and training loss. Specifically, as expected, standard dithering achieves the quickest run time; however, exponential dithering is slightly slower but achieves a better convergence similar to no quantization. Notably, exponential dithering can preserve better convergence than other compression methods. Statistics of the final loss values can be found in Appendix D.

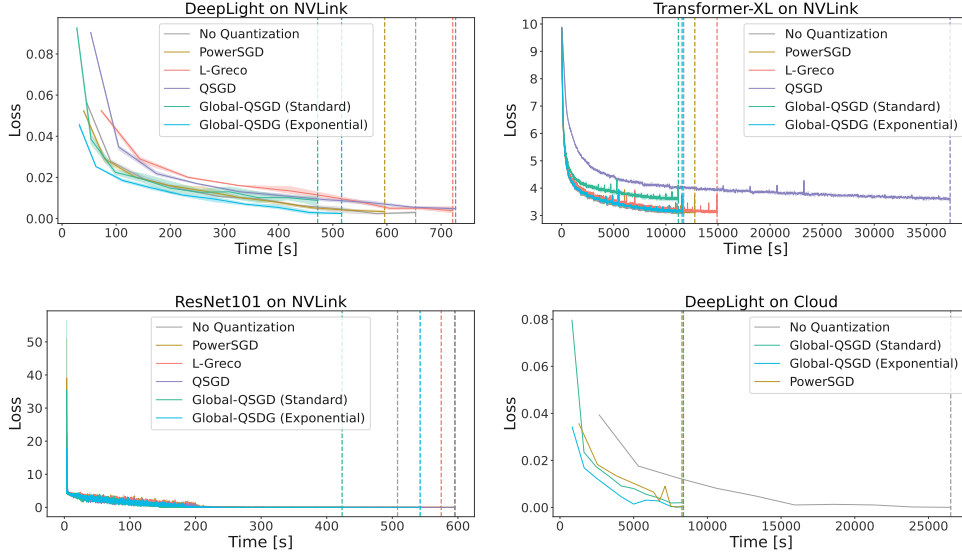


Figure 2: Training behaviors across three benchmarks. Vertical dashed lines represent the completion times of each method. The solid line is the average loss across three random seeds, and the shadow represents the range between max and min.

Generalization. Instead of training loss, we also evaluate models with domain-specific metrics on the test sets.¹¹ Table 3 shows that both standard dithering and exponential dithering can preserve the same level of generalization ability as no quantization.

	DeepLight AUC	ResNet50 Top 1	TransformerXL PPL
No Quantization	0.676 ± 0.010	$76.87\% \pm 0.04\%$	23.75 ± 0.110
Standard Dithering	0.698 ± 0.003	$76.46\% \pm 0.25\%$	33.12 ± 0.705
Exponential Dithering	0.687 ± 0.010	$76.55\% \pm 0.03\%$	24.35 ± 0.124

Table 3: Validation Metrics

Limitations. The current implementation is not completely optimized. We make use of the NCCL P2P API and there are synchronous invocations that prevent pipelining of opportunities for further overlapping compression and communication.

8 Conclusion

We introduced a novel family of quantization operators for distributed learning based on global normalization. This enables the use of fast Allreduce communication and is backed by sound theory. Through extensive experiments, we showed that our proposed method yields fast convergence in real-world deployments. In particular, we demonstrated that Global-QSGD with exponential dithering $\text{Global-}\mathcal{E}_s^{q,p}$ achieves the best balance between the variance caused by compression and the speed of convergence.

¹¹We use the full Imagenet test set instead of MiniImagenet because it is more suitable to evaluate generalization ability. We use ResNet50 instead of ResNet101 to reduce the training time.

References

- [1] Geoffrey Hinton, Oriol Vinyals, Jeff Dean, et al. Distilling the knowledge in a neural network. *arXiv preprint arXiv:1503.02531*, 2(7), 2015.
- [2] Kaiming He, Xiangyu Zhang, Shaoqing Ren, and Jian Sun. Deep residual learning for image recognition. In *Proceedings of the IEEE conference on computer vision and pattern recognition*, pages 770–778, 2016.
- [3] Gao Huang, Zhuang Liu, Laurens Van Der Maaten, and Kilian Q Weinberger. Densely connected convolutional networks. In *Proceedings of the IEEE conference on computer vision and pattern recognition*, pages 4700–4708, 2017.
- [4] Jacob Devlin, Ming-Wei Chang, Kenton Lee, and Kristina Toutanova. Bert: Pre-training of deep bidirectional transformers for language understanding. *arXiv preprint arXiv:1810.04805*, 2018.
- [5] Martín Abadi, Paul Barham, Jianmin Chen, Zhifeng Chen, Andy Davis, Jeffrey Dean, Matthieu Devin, Sanjay Ghemawat, Geoffrey Irving, Michael Isard, et al. TensorFlow: A System for Large-Scale Machine Learning. In *12th USENIX symposium on operating systems design and implementation (OSDI 16)*, pages 265–283, 2016.
- [6] Jeffrey Dean, Greg Corrado, Rajat Monga, Kai Chen, Matthieu Devin, Mark Mao, Marc’aurelio Ranzato, Andrew Senior, Paul Tucker, Ke Yang, et al. Large scale distributed deep networks. *Advances in neural information processing systems*, 25, 2012.
- [7] Norman P Jouppi, Cliff Young, Nishant Patil, David Patterson, Gaurav Agrawal, Raminder Bajwa, Sarah Bates, Suresh Bhatia, Nan Boden, Al Borchers, et al. In-datacenter performance analysis of a tensor processing unit. In *Proceedings of the 44th annual international symposium on computer architecture*, pages 1–12, 2017.
- [8] Amedeo Sapia, Marco Canini, Chen-Yu Ho, Jacob Nelson, Panos Kalnis, Changhoon Kim, Arvind Krishnamurthy, Masoud Moshref, Dan R. K. Ports, and Peter Richtárik. Scaling distributed machine learning with in-network aggregation. In *The 18th USENIX Symposium on Networked Systems Design and Implementation*, 2021.
- [9] Thijs Vogels, Sai Praneeth Karimireddy, and Martin Jaggi. Powersgd: Practical low-rank gradient compression for distributed optimization. *Advances in Neural Information Processing Systems*, 32, 2019.
- [10] Saurabh Agarwal, Hongyi Wang, Shivaram Venkataraman, and Dimitris Papailiopoulos. On the utility of gradient compression in distributed training systems. *Proceedings of Machine Learning and Systems*, 4, 2022.
- [11] Soojeong Kim, Gyeong-In Yu, Hojin Park, Sungwoo Cho, Eunji Jeong, Hyeonmin Ha, Sanha Lee, Joo Seong Jeong, and Byung-Gon Chun. Parallax: Sparsity-aware Data Parallel Training of Deep Neural Networks. In *EuroSys*, 2019.
- [12] Frank Seide, Hao Fu, Jasha Droppo, Gang Li, and Dong Yu. 1-bit stochastic gradient descent and application to data-parallel distributed training of speech DNNs. In *Interspeech 2014*, September 2014.
- [13] Nikko Strom. Scalable distributed DNN training using commodity GPU cloud computing. In *Sixteenth Annual Conference of the International Speech Communication Association*, 2015.
- [14] Dan Alistarh, Demjan Grubic, Jerry Li, Ryota Tomioka, and Milan Vojnovic. QSGD: Communication-Efficient SGD via Gradient Quantization and Encoding. In *Advances in Neural Information Processing Systems (NeurIPS)*, 2017.
- [15] Wei Wen, Cong Xu, Feng Yan, Chunpeng Wu, Yandan Wang, Yiran Chen, and Hai Li. Terngrad: Ternary gradients to reduce communication in distributed deep learning. In *Advances in Neural Information Processing Systems (NeurIPS)*, pages 1509–1519, 2017.

- [16] Suyog Gupta, Ankur Agrawal, Kailash Gopalakrishnan, and Pritish Narayanan. Deep learning with limited numerical precision. In *International Conference on Machine Learning (ICML)*, pages 1737–1746, 2015.
- [17] T. Na, J. H. Ko, J. Kung, and S. Mukhopadhyay. On-chip training of recurrent neural networks with limited numerical precision. In *2017 International Joint Conference on Neural Networks (IJCNN)*, pages 3716–3723, May 2017. doi: 10.1109/IJCNN.2017.7966324.
- [18] Konstantin Mishchenko, Eduard Gorbunov, Martin Takáč, and Peter Richtárik. Distributed learning with compressed gradient differences. *arXiv preprint arXiv:1901.09269*, 2019.
- [19] Samuel Horváth, Chen-Yu Ho, Ludovít Horváth, Atal Narayan Sahu, Marco Canini, and Peter Richtárik. Natural compression for distributed deep learning. *arXiv preprint arXiv:1905.10988*, 2019.
- [20] Ananda Theertha Suresh, Felix X. Yu, Sanjiv Kumar, and H. Brendan McMahan. Distributed mean estimation with limited communication. In *International Conference on Machine Learning (ICML)*, 2017.
- [21] Jakub Konečný and Peter Richtárik. Randomized distributed mean estimation: accuracy vs communication. *Frontiers in Applied Mathematics and Statistics*, 4(62):1–11, 2018.
- [22] Dan Alistarh, Torsten Hoefler, Mikael Johansson, Nikola Konstantinov, Sarit Khirirat, and Cedric Renggli. The convergence of sparsified gradient methods. In *Advances in Neural Information Processing Systems (NeurIPS)*, volume 31, pages 5973–5983, 2018.
- [23] Sebastian U Stich, Jean-Baptiste Cordonnier, and Martin Jaggi. Sparsified SGD with memory. In *Advances in Neural Information Processing Systems (NeurIPS)*, pages 4447–4458, 2018.
- [24] Hongyi Wang, Scott Sievert, Shengchao Liu, Zachary Charles, Dimitris Papailiopoulos, and Stephen Wright. Atomo: Communication-efficient learning via atomic sparsification. *Advances in Neural Information Processing Systems (NeurIPS)*, 31:9850–9861, 2018.
- [25] Peter Richtárik and Martin Takáč. Distributed coordinate descent method for learning with big data. *Journal of Machine Learning Research (JMLR)*, 17(75):1–25, 2016.
- [26] Olivier Fercoq, Zheng Qu, Peter Richtárik, and Martin Takáč. Fast distributed coordinate descent for minimizing non-strongly convex losses. *IEEE International Workshop on Machine Learning for Signal Processing*, 2014.
- [27] Konstantin Mishchenko, Filip Hanzely, and Peter Richtárik. 99% of worker-master communication in distributed optimization is not needed. In *Conference on Uncertainty in Artificial Intelligence*, pages 979–988, 2020.
- [28] Konstantin Mishchenko, Bokun Wang, Dmitry Kovalev, and Peter Richtárik. Intsgd: Adaptive floatless compression of stochastic gradients. In *International Conference on Learning Representations*, 2021.
- [29] Sai Praneeth Karimireddy, Quentin Rebjock, Sebastian Stich, and Martin Jaggi. Error feedback fixes signsgd and other gradient compression schemes. In *International Conference on Machine Learning*, pages 3252–3261. PMLR, 2019.
- [30] Eduard Gorbunov, Filip Hanzely, and Peter Richtárik. A unified theory of SGD: Variance reduction, sampling, quantization and coordinate descent. In *International Conference on Artificial Intelligence and Statistics (AISTATS)*, pages 680–690, 2020.
- [31] Jeremy Bernstein, Yu-Xiang Wang, Kamyar Azizzadenesheli, and Animashree Anandkumar. signsgd: Compressed optimisation for non-convex problems. In *International Conference on Machine Learning*, pages 560–569. PMLR, 2018.
- [32] Aleksandr Beznosikov, Samuel Horváth, Peter Richtárik, and Mher Safaryan. On biased compression for distributed learning. *arXiv preprint arXiv:2002.12410*, 2020.

- [33] Peter Richtárik, Igor Sokolov, and Ilyas Fatkhullin. EF21: A new, simpler, theoretically better, and practically faster error feedback. In *Advances in Neural Information Processing Systems (NeurIPS)*, 2021.
- [34] Samuel Horváth and Peter Richtárik. A better alternative to error feedback for communication-efficient distributed learning. In *International Conference on Learning Representations (ICLR)*, 2021.
- [35] Cong Xie, Shuai Zheng, Sanmi Koyejo, Indranil Gupta, Mu Li, and Haibin Lin. Cser: Communication-efficient sgd with error reset. *Advances in Neural Information Processing Systems*, 33:12593–12603, 2020.
- [36] Priya Goyal, Piotr Dollár, Ross B. Girshick, Pieter Noordhuis, Lukasz Wesolowski, Aapo Kyrola, Andrew Tulloch, Yangqing Jia, and Kaiming He. Accurate, large minibatch SGD: training ImageNet in 1 hour. *CoRR*, abs/1706.02677, 2017.
- [37] Ohad Shamir, Nati Srebro, and Tong Zhang. Communication-efficient distributed optimization using an approximate Newton-type method. In *International Conference on Machine Learning (ICML)*, volume 32, pages 1000–1008, 2014.
- [38] Sashank J. Reddi, Jakub Konečný, Peter Richtárik, Barnabás Póczos, and Alexander J. Smola. AIDE: Fast and communication efficient distributed optimization. *CoRR*, abs/1608.06879, 2016.
- [39] Ryan McDonald, Mehryar Mohri, Nathan Silberman, Dan Walker, and Gideon S. Mann. Efficient large-scale distributed training of conditional maximum entropy models. In *Advances in Neural Information Processing Systems (NeurIPS)*, pages 1231–1239, 2009.
- [40] Martin Zinkevich, Markus Weimer, Lihong Li, and Alex J. Smola. Parallelized stochastic gradient descent. In *Advances in Neural Information Processing Systems (NeurIPS)*, pages 2595–2603, 2010.
- [41] Yang You, Zhao Zhang, Cho-Jui Hsieh, James Demmel, and Kurt Keutzer. Imagenet training in minutes. In *Proceedings of the 47th International Conference on Parallel Processing*, pages 1–10, 2018.
- [42] Sebastian U Stich. Local SGD converges fast and communicates little. In *International Conference on Learning Representations (ICLR)*, 2019.
- [43] Konstantin Mishchenko, Grigory Malinovsky, Sebastian Stich, and Peter Richtárik. ProxSkip: Yes! Local gradient steps provably lead to communication acceleration! Finally! *arXiv preprint arXiv:2202.09357*, 2022.
- [44] Sarit Khirirat, Hamid Reza Feyzmahdavian, and Mikael Johansson. Distributed learning with compressed gradients. *arXiv preprint arXiv:1806.06573*, 2018.
- [45] Jean-Baptiste Cordonnier. Convex optimization using sparsified stochastic gradient descent with memory. Technical report, École Polytechnique Fédérale de Lausanne, 2018.
- [46] Anastasia Koloskova, Sebastian Stich, and Martin Jaggi. Decentralized stochastic optimization and gossip algorithms with compressed communication. In *International Conference on Machine Learning (ICML)*, pages 3478–3487, 2019.
- [47] Ali Ramezani-Kebrya, Fartash Faghri, Ilya Markov, Vitalii Aksenov, Dan Alistarh, and Daniel M. Roy. NUQSGD: Provably communication-efficient data-parallel SGD via nonuniform quantization. *Journal of Machine Learning Research (JMLR)*, 22(114):1–43, 2021.
- [48] Rajeev Thakur, Rolf Rabenseifner, and William Gropp. Optimization of collective communication operations in mpich. *The International Journal of High Performance Computing Applications*, 19(1):49–66, 2005.
- [49] Mohammadreza Alimohammadi, Iliia Markov, Elias Frantar, and Dan Alistarh. L-greco: An efficient and general framework for layerwise-adaptive gradient compression. *arXiv preprint arXiv:2210.17357*, 2022.

A Proofs

In this section, we include complete proofs of the claims made in the main paper.

A.1 Proof of Lemma 2.3

Firstly, we show unbiasedness.

$$\mathbf{E}[\mathcal{Q}(\mathbf{x})] = \mathbf{E}\left[\frac{1}{n} \sum_{i=1}^n \mathcal{C}_i(x_i)\right] = \frac{1}{n} \sum_{i=1}^n \mathbf{E}[\mathcal{C}_i(x_i)] \stackrel{(2)}{=} \frac{1}{n} \sum_{i=1}^n x_i = \bar{\mathbf{x}}.$$

For the variance,

$$\mathbf{E}[\|\mathcal{Q}(\mathbf{x}) - \bar{\mathbf{x}}\|_2^2] = \mathbf{E}\left[\left\|\frac{1}{n} \sum_{i=1}^n \mathcal{C}_i(x_i) - x_i\right\|_2^2\right] = \frac{1}{n^2} \sum_{i=1}^n \mathbf{E}[\|\mathcal{C}_i(x_i) - x_i\|_2^2] \stackrel{(2)}{\leq} \frac{\omega}{n} \frac{1}{n} \sum_{i=1}^n \|x_i\|_2^2,$$

where the second equality is due to independence and zero mean of each summand.

A.2 Proof of Lemma 3.2

It is easy to that such operator is unbiased since $\mathbf{E}[(\xi(y_i))] = (\xi(y_i))_j$ by construction. Therefore,

$$\begin{aligned} \mathbf{E}[\text{Global-}\mathcal{Q}_l^{q,p}(\mathbf{x})] &\stackrel{(5)}{=} \mathbf{E}\left[\|\mathbf{x}\|_{q,p} \frac{1}{n} \sum_{i=1}^n \text{sign}(x_i) \circ \xi_i(y_i)\right] = \|\mathbf{x}\|_{q,p} \frac{1}{n} \sum_{i=1}^n \text{sign}(x_i) \circ \mathbf{E}[\xi_i(y_i)] \\ &\stackrel{(6)}{=} \|\mathbf{x}\|_{q,p} \frac{1}{n} \sum_{i=1}^n \text{sign}(x_i) \circ y_i = \|\mathbf{x}\|_{q,p} \frac{1}{n} \sum_{i=1}^n \text{sign}(x_i) \circ \frac{x_i}{\|\mathbf{x}\|_{q,p}} = \bar{\mathbf{x}}. \end{aligned}$$

Furthermore, note that for Global- \mathcal{Q} , the local compression operators do not belong to $\mathbb{U}^n(\omega)$ for any $\omega > 0$ due to its dependence on \mathbf{x} .

To obtain the variance bound, we show that it is sufficient to look at $n = 1$, which corresponds to the unbiased compressor (Definition 2.1) due to the following property.

$$\begin{aligned} \mathbf{E}[\|\text{Global-}\mathcal{Q}_l^{q,p}(\mathbf{x}) - \bar{\mathbf{x}}\|_2^2] &\stackrel{(5)}{=} \mathbf{E}\left[\left\|\|\mathbf{x}\|_{q,p} \frac{1}{n} \sum_{i=1}^n \left(\text{sign}(x_i) \circ \xi_i(y_i) - \frac{x_i}{\|\mathbf{x}\|_{q,p}}\right)\right\|_2^2\right] \\ &= \frac{1}{n^2} \sum_{i=1}^n \mathbf{E}\left[\left\|\|\mathbf{x}\|_{q,p} \left(\text{sign}(x_i) \circ \xi_i(y_i) - \frac{x_i}{\|\mathbf{x}\|_{q,p}}\right)\right\|_2^2\right] \\ &= \frac{1}{n^2} \mathbf{E}\left[\|\|\mathbf{x}\|_{q,p} \text{sign}(\mathbf{x}) \circ \xi(\mathbf{y}) - \mathbf{x}\|_2^2\right] \\ &= \frac{1}{n^2} \mathbf{E}\left[\|\mathcal{Q}_l^{q,p}(\mathbf{x}) - \mathbf{x}\|_2^2\right], \end{aligned}$$

where the second inequality is due to independence of $\{\xi_i\}$. If we can show that $\mathcal{Q}_l^{q,p}(\mathbf{x}) \in \mathbb{U}^{1,nd}(\omega)$, then

$$\mathbf{E}[\|\text{Global-}\mathcal{Q}_l^{q,p}(\mathbf{x}) - \bar{\mathbf{x}}\|_2^2] = \frac{1}{n^2} \mathbf{E}[\|\mathcal{Q}_l^{q,p}(\mathbf{x}) - \mathbf{x}\|_2^2] \leq \frac{\omega}{n^2} \|\mathbf{x}\|_{2,2}^2 = \frac{\omega}{n} \frac{1}{n} \sum_{i=1}^n \|x_i\|_2^2,$$

which implies $\theta = \omega/n$.

A.3 Proof of Theorem 3.3

The results provided in the theorem are direct consequences of Lemma 3.2 combined with known one-node results of Alistarh et al. [14], Horváth et al. [19]. For the variance part, we firstly use the second part of Lemma 3.2, which shows that if $\mathcal{Q}_l^{q,p} \in \mathcal{C}(\omega)$ then $\text{Global-}\mathcal{Q}_l^{q,p} \in \mathbb{U}^{n,d}(\theta)$ with $\theta = \omega/n$. Secondly, we apply $n = 1$ results of [19, Theorem 7] and [14, Theorem 3.4] combined

with the norm inequality that states $\|\mathbf{x}\|_{q,p} \leq \|\mathbf{x}\|_{2,2}$ for $p, q \geq 2$. The claim about sparsity with $p = q = 2$ follows from the first part of Lemma 3.2, which implies that the number of non-zero elements of $\text{Global-}\mathcal{Q}_l^{q,p}$ before aggregation is the same as $\mathcal{Q}_l^{q,p}$. The rest of the proof for $\mathcal{L}_s^{2,2}$ follows directly from [14, Lemma 3.1]. For $\mathcal{E}_s^{2,2}$, one can also directly apply [14, Lemma 3.1] using the fact that the length of the first segment $[l_s, l_{s-1}]$ is $1/2^{s-1}$.

A.4 Proof for Equation 8

The condition of performance gain is per-batch training time after applying Global-QSGD is less than the per-batch training time without quantization, which is Equation (??) > Equation (??):

$$\begin{aligned} 2 \log(N)\alpha + 2 \frac{\log(N)S}{\beta} + \frac{\log(N)S}{\gamma} &> 2 \log(N)\alpha + 2 \frac{\log(N)\hat{S}}{\beta} + \frac{\log(N)\hat{S}}{\hat{\gamma}} + \delta S \\ 2 \frac{S}{\beta} + \frac{S}{\gamma} &> 2 \frac{\hat{S}}{\beta} + \frac{\hat{S}}{\hat{\gamma}} \\ 2 \frac{\rho}{\beta} + \frac{\rho}{\gamma} &> 2 \frac{1}{\beta} + \frac{1}{\hat{\gamma}} \\ \beta &< 2 \frac{\gamma \hat{\gamma} (\rho - 1)}{\gamma - \rho \hat{\gamma}} \\ \beta &< \frac{2\omega(\rho - 1)}{1 - \omega\rho} \gamma \end{aligned}$$

Then we substitute $\rho = 4$:

$$\beta < \frac{6\omega}{1 - 4\omega} \gamma$$

A.5 Convergence Analysis

We first look at the standard local compression. Our gradient estimator has the following form $\frac{1}{n} \sum_{i=1}^n C_i(\nabla f_i(x, \xi_i))$ where $C_1, C_2, \dots, C_n \in \mathbb{U}^n(\omega)$ are independent. We also assume $\{\xi_i\}$ and $\{C_i\}$ to be independent. Therefore, using variance bound, unbiasedness, independence, and the tower property of expectation, we obtain

$$\begin{aligned} \mathbf{E} \left[\left\| \frac{1}{n} \sum_{i=1}^n C_i(\nabla f_i(x, \xi_i)) - \nabla f(x) \right\|_2^2 \right] &= \\ \frac{1}{n^2} \sum_{i=1}^n \mathbf{E} \left[\|C_i(\nabla f_i(x, \xi_i)) - \nabla f_i(x)\|_2^2 \right] &= \\ = \frac{1}{n^2} \sum_{i=1}^n \left(\mathbf{E} \left[\|C_i(\nabla f_i(x, \xi_i)) - \nabla f_i(x, \xi_i)\|_2^2 \right] \right) &= \\ + \frac{1}{n^2} \sum_{i=1}^n \left(\mathbf{E} \left[\|\nabla f_i(x, \xi_i) - \nabla f_i(x)\|_2^2 \right] \right) &= \\ \leq \frac{1}{n^2} \sum_{i=1}^n \left(\omega \mathbf{E} \left[\|\nabla f_i(x, \xi_i)\|_2^2 \right] \right) &= \\ + \frac{1}{n^2} \sum_{i=1}^n \left(\mathbf{E} \left[\|\nabla f_i(x, \xi_i) - \nabla f_i(x)\|_2^2 \right] \right) &= \\ = \frac{\omega}{n} \frac{1}{n} \sum_{i=1}^n \mathbf{E} \left[\|\nabla f_i(x)\|_2^2 \right] &= \\ + \frac{\omega + 1}{n} \frac{1}{n} \sum_{i=1}^n \mathbf{E} \left[\|\nabla f_i(x, \xi_i) - \nabla f_i(x)\|_2^2 \right]. & \end{aligned}$$

Analogously, we can derive that for $\mathcal{Q} \in \mathbb{U}^{n,d}(\theta)$, we have

$$\begin{aligned} \mathbf{E} \left[\|\mathcal{Q}(\nabla f_1(x, \xi_i), \dots, \nabla f_1(x, \xi_i)) - \nabla f(x)\|_2^2 \right] &\leq \\ \theta \frac{1}{n} \sum_{i=1} \mathbf{E} \left[\|\nabla f_i(x)\|_2^2 \right] &+ \left(\theta + \frac{1}{n} \right) \frac{1}{n} \sum_{i=1} \mathbf{E} \left[\|\nabla f_i(x, \xi_i) - \nabla f_i(x)\|_2^2 \right]. \end{aligned}$$

B Reduce function for Global- $\mathcal{E}_s^{q,p}$

Since our reduce function acts element-wise, we only consider here a one-dimensional case. We provide complete pseudo-code and vectorized implementation in Algorithm 2.

Algorithm 2 Reduce function for Global- \mathcal{E}_s^{1,q,p_s}

```

1: Input:  $(\text{sign}_1, e_1), (\text{sign}_2, e_2), m \stackrel{\text{def}}{=} s + 1$ 
2:  $k = -\lfloor \log((2^{-m} + [p - 2^{-m}]_+)) \rfloor$ , where  $p \sim \text{Unif}[0, 1]^d$  // can be precomputed
3:  $e\_1\_is\_not\_zero = \mathbf{1}(e_1 > 0)$ 
4:  $e\_2\_is\_not\_zero = \mathbf{1}(e_2 > 0)$ 
5:  $e\_2\_is\_not\_zero = 1 - e\_2\_is\_not\_zero$ 
6:  $\text{sign}_{12} = \text{sign}_1 \text{sign}_2 e\_1\_is\_not\_zero e\_2\_is\_not\_zero$ 
7:  $\text{diff} = |e_1 - e_2| - (1 - \text{sign}_{12})/2$ 
8:  $\text{leq} = (\mathbf{1}(e_1 \leq e_2) + e\_2\_is\_zero) e\_1\_is\_not\_zero$ 
9:  $\text{non\_zero} = 1 - \mathbf{1}(e_1 = e_2 \text{ and } \text{sign}_{12} = -1)$ 
10:  $\text{sign}_{\text{result}} = \text{sign}_1 \text{leq} + \text{sign}_2 (1 - \text{leq})$ 
11:  $e_{\text{result}} = (e_1 \text{leq} + e_2 (1 - \text{leq}) - \text{sign}_{12} \mathbf{1}(k > \text{diff})) \text{non\_zero}$ 
12: Output:  $\text{sign}_{\text{result}}, e_{\text{result}}$ 

```

Before calling the compression operator and the reduce function, we divide all values by $2n$, where n is the number of nodes, to ensure that the maximum power of two we encounter during the aggregation is -1 that corresponds to $1/2 = 2^{-1}$. Therefore, all the encountered exponents during the aggregation are guaranteed to be negative. This way, we can dedicate exponent zero to the actual zero instead of 2^0 . Next, we define the representation, which we use during the aggregation when calling the reduce function after applying exponential dithering locally. Let $\text{sign} \in \{-1, +1\}^{12}$ be the sign and $e \in \{\mathcal{N}^+ \cup \{0\}\}$ be the communicated non-negative integer-valued exponents. Then, then real number x that corresponds to the pair (sign, e) is defined as

$$x = \begin{cases} 0, & \text{if } e = 0, \\ \text{sign } 2^{-e}, & \text{otherwise.} \end{cases} \quad (9)$$

We proceed with the derivation for the reduce function. Let $x_1, x_2 \in \mathbb{R}$ represented by $(\text{sign}_1, e_1), (\text{sign}_2, e_2)$, respectively, be the values to be summed using reduce function. To facilitate efficient rounding, let us define

$$k = -\left\lfloor \log\left(2^{-m} + [p - 2^{-m}]_+\right) \right\rfloor,$$

where $p \sim \text{Unif}[0, 1]$ is a sample from the uniform distribution on the interval $[0, 1]$, $m \stackrel{\text{def}}{=} s + 1$ is the maximum difference $|e_1 - e_2|$ that can appear during the aggregation, and $[x]_+ \stackrel{\text{def}}{=} \max\{0, x\}$. Note that the support set for k is $\{0, 1, \dots, m\}$, and for $b \in \{0, 1, \dots, m-1\}$, it holds

$$\text{Prob}(k > b) = \text{Prob}(-k < -b) = \text{Prob}(p < 2^{-b}) = 2^{-b}.$$

¹²Zeros have any sign.

Without loss of generality, we assume that $\text{sign}_1 = 1$ and $0 < e_1 \geq e_2$. We discuss how to handle the case e_1 at the end of this section. If $\text{sign}_2 = 1$, then

$$C_{\text{nat}}(2^{-e_1} + 2^{-e_2}) = \begin{cases} 2^{-e_1+1}, & \text{w.p. } 2^{e_1-e_2}, \\ 2^{-e_1}, & \text{w.p. } 1 - 2^{e_1-e_2}, \end{cases}$$

where w.p. stands for with probability. We note that

$$p < 2^{e_1-e_2} \iff k > e_2 - e_1.$$

Therefore,

$$C_{\text{nat}}(2^{-e_1} + 2^{-e_2}) = \begin{cases} 2^{-e_1+1}, & \text{if } k > e_2 - e_1, \\ 2^{-e_1}, & \text{otherwise.} \end{cases}$$

Analogically, if $\text{sign}_2 = -1$

$$C_{\text{nat}}(2^{-e_1} - 2^{-e_2}) = \begin{cases} 0, & \text{if } e_1 = e_2 \\ \begin{cases} 2^{-e_1-1}, & \text{w.p. } 2^{e_2-e_1-1}, \\ 2^{-e_1}, & \text{w.p. } 1 - 2^{e_2-e_1-1}, \end{cases} & \text{otherwise.} \end{cases}$$

Equivalently, we can write

$$C_{\text{nat}}(2^{-e_1} - 2^{-e_2}) = \begin{cases} 0, & \text{if } e_1 = e_2 \\ \begin{cases} 2^{-e_1-1}, & \text{w.p. } k > e_2 - e_1 - 1, \\ 2^{-e_1}, & \text{w.p. } k > e_2 - e_1 - 1, \end{cases} & \text{otherwise.} \end{cases}$$

In general case, we compare k to the following quantity

$$\text{diff} = |e_1 - e_2| - (1 - \text{sign}_{12}) // 2,$$

where $\text{sign}_{12} \stackrel{\text{def}}{=} \text{sign}_1 \text{sign}_2 \in \{-1, 1\}$ and $//$ corresponds to the integer division. It is easy to check that the above quantity recovers all the cases discussed above. To determine which exponent is smaller, we use $\text{leq} = \mathbf{1}(e_1 \leq e_2) \in \{0, 1\}$, where $\mathbf{1}$ is the indicator function. Finally, to filter out the case of the different signs and the same exponent, we use $\text{non_zero} \stackrel{\text{def}}{=} 1 - \mathbf{1}(e_1 = e_2 \text{ and } \text{sign}_{12} = -1) \in \{0, 1\}$. Then, we obtain the resulting sign and exponent as

$$\begin{aligned} \text{sign}_{\text{result}} &= \text{sign}_1 \text{leq} + \text{sign}_2(1 - \text{leq}) \\ e_{\text{result}} &= (e_1 \text{leq} + e_2(1 - \text{leq}) - \text{sign}_{12} \mathbf{1}(k > \text{diff})) \text{non_zero}. \end{aligned}$$

To incorporate zeros, we first define the following variables to identify zeros

$$\begin{aligned} e_1_is_not_zero &= \mathbf{1}(e_1 > 0) \\ e_2_is_not_zero &= \mathbf{1}(e_2 > 0) \\ e_2_is_not_zero &= 1 - e_2_is_zero. \end{aligned}$$

In the case of at least one of the exponents being zero, we do not change the exponents by adding or subtracting zero. This can be achieved by redefine sign_{12} to

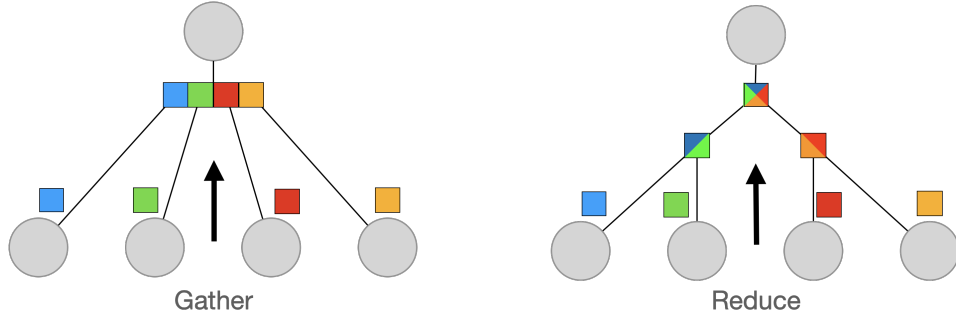
$$\text{sign}_{12} \stackrel{\text{def}}{=} \text{sign}_1 \text{sign}_2 e_1_is_not_zero e_2_is_not_zero \in \{-1, 0, 1\}.$$

Furthermore, we need to redefine leq to account for zeros. This can be achieved by

$$\text{leq} \stackrel{\text{def}}{=} (\mathbf{1}(e_1 \leq e_2) + e_2_is_zero) e_1_is_not_zero.$$

This concludes our construction of the reduce function for the exponential dithering.

C Visualization of Gather and Reduce



D Training Losses

	DeepLight	ResNet50	TransformerXL
No Quantization	$2.89 \pm 0.46 * 10^3$	6.29 ± 0.077	3.09 ± 0.006
Standard Dithering	$3.82 \pm 1.67 * 10^3$	6.21 ± 0.054	3.60 ± 0.032
Exponential Dithering	$2.43 \pm 0.15 * 10^3$	6.21 ± 0.063	3.14 ± 0.015
L-Greco	$1.10 \pm 0.48 * 10^4$	6.23 ± 0.051	3.12 ± 0.006

Table 4: Training Losses